

## Spectroscopic study on water diffusion in poly(lactic acid) film†

Ying Jin, Wei Wang and Zhaohui Su\*

Received 24th April 2012, Accepted 16th June 2012

DOI: 10.1039/c2py20259j

The diffusion of water in biocompatible semicrystalline poly(lactic acid) (PLA) is investigated using time-resolved ATR-FTIR. There are three different states of water molecules diffusing into the film. Using a 2D correlation analysis, the diffusion process and the role of different functional groups on diffusion is obtained. First, the moderately strongly bound water forms a hydrogen bond with  $\text{C=O}$ . Then, the water diffuses into free volume (microvoids) and strong hydrogen bonds are formed between two  $\text{C=O}$  groups and water. The conformations of semicrystalline PLA change during the diffusion process and recover after re-drying. In addition, water first interacts with amorphous segments and then interacts with crystalline segments.

### Introduction

As an environmentally friendly, biodegradable and biocompatible crystalline polymer, poly(lactic acid) (PLA) has attracted significant interest in recent years. PLA is environmentally and economically appropriate because it can be produced from renewable resources such as corn, and it degrades into lactic acid, which is nontoxic and bioresorbable, and is naturally present in the human body. Furthermore, PLA has many advantages in its inherent properties, such as biocompatibility, processability, and good mechanical properties comparable to those of commercial polymers.<sup>1–4</sup> Therefore PLA has found application in biomedical and pharmaceutical fields, such as bone fixation materials, controlled drug delivery systems,<sup>5</sup> bioabsorbable surgical sutures,<sup>6,7</sup> and blood vessel repair.<sup>8</sup> In addition, some traditional applications of PLA have been explored. It has shown potential as a substitute for common fossil fuel based thermoplastics and has been used in the production of plastic bags, films, and fibers.<sup>9,10</sup>

In all of these applications, in particular as biomedical material, PLA is often in contact with water, and the water absorbed by the polymer inevitably impacts on the performance of the material. The chemical and physical properties of polymeric materials can transform accordingly<sup>11</sup> and water even causes degradation sometimes. It has been reported that hydrolysis of the ester linkages in the aliphatic chains of PLA causes its degradation.<sup>12</sup> While the sorption of water is an important factor that influences the performance and the rate of degradation of PLA, the process is not straightforward. In some cases water was

assumed to diffuse into the free volume of the polymer matrix, while in others water molecules may couple with certain hydrophilic groups (*e.g.* carbonyl or oxygen) to form hydrogen bonds of different strength with the polymer.<sup>13–15</sup> So far the molecular mechanism of water diffusion in the PLA matrix is not well established.<sup>16</sup> In addition, influence of PLA crystallinity on water diffusion and degradation behavior is distinct from other semicrystalline polymers and the literature is also inconsistent.<sup>17–20</sup> Therefore, it is necessary to study water diffusion in PLA at a molecular level.

Attenuated total reflection Fourier transform infrared spectroscopy (ATR-FTIR) is a convenient, rapid, and accurate technique and requires minimum sample handling, therefore is particularly suitable for probing the dynamic diffusion behavior of small molecules in polymer films.<sup>21–26</sup> The spectral data can be processed by the generalized two-dimensional (2D) correlation analysis, which improves the spectral resolution of highly overlapped FT-IR bands<sup>27–29</sup> and identifies the specific sequence of certain spectral intensity changes occurring in the period of the progress of a significant controlling physical variable in the dynamic analysis.<sup>27,29–31</sup> ATR-FTIR in conjunction with 2D correlation analysis has proved a powerful tool for studying water diffusion in various polymer matrices.<sup>31–35</sup>

In this work, time-resolved ATR-FTIR is employed to monitor the diffusion of water into PLA films of different morphologies, and the interactions between water molecules and PLA chains are investigated.

### Experimental

#### Sample preparation

Poly(lactic acid) (PLA) was a commercial product purchased from Natureworks (PLA 4032D, 98% L-lactide content,  $M_w \sim 250k$ , PDI  $\sim 1.70$ ) and used as received. Dichloromethane was purchased from Beijing Chemicals Co. and used as received.

State Key Laboratory of Polymer Physics and Chemistry, Changchun Institute of Applied Chemistry, Chinese Academy of Sciences, 5625 Renmin Street, Changchun 130022, People's Republic of China. E-mail: zhsu@ciac.jl.cn; Fax: +86-431-85262126; Tel: +86-431-85262854

† Electronic supplementary information (ESI) available: morphology of PLA films determined by DSC and FTIR, and 2D synchronous spectra for the water diffusion process. See DOI: 10.1039/c2py20259j

PLA samples were prepared by casting a dichloromethane solution (10% w/v) onto clean glass slides or KBr tablets, and the films were maintained at room temperature for 36 h to allow the evaporation of the residual solvent. The films cast on glass substrates were peeled off from the substrates. In a Linkam THMS 600 hot-stage under nitrogen atmosphere, the films on KBr tablets were first heated to 200 °C to a complete melt, and then quickly cooled to 120 °C and maintained at this temperature for 90 min. Then the films were cooled to room temperature, and free-standing PLA films were obtained by dissolving the KBr tablets from the bottom in a water bath. All films were maintained under vacuum at 40 °C for 24 h before ATR-FTIR measurements. Ultrapure water (18.2 MΩ cm) obtained from a Millipore Simplicity unit was used for water diffusion measurements.

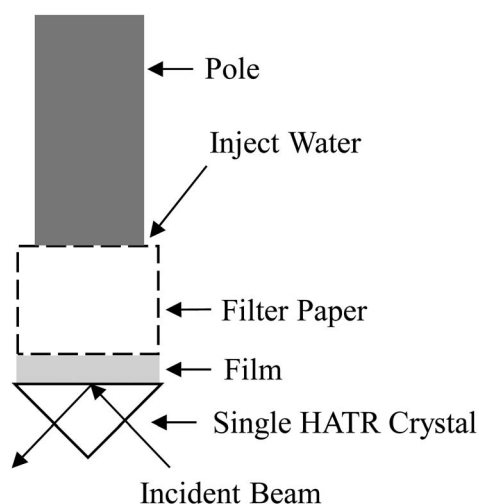
### Diffusion measurements by time-resolved ATR-FTIR

The thickness of all the films was greater than 10 μm. Time-resolved ATR-FTIR measurements were carried out at room temperature on a Bruker Vertex 70 spectrometer equipped with a DTGS detector and a single-reflection ATR accessory (ZnSe crystal, 45°). The ATR crystal covered by the polymer film with several layers of overlaying filter paper was mounted in the ATR cell, as shown in Scheme 1, and then 50 μL of water was injected into the filter paper while data acquisition was initiated.

For the diffusion process, 16 scans were added together for each spectrum, with a 15 s time interval before the next spectral acquisition. All spectra were collected at 4 cm<sup>-1</sup> resolution in the range of 4000–650 cm<sup>-1</sup>, and baseline-corrected using the OPUS 5.0 software. Curve fitting was performed using the Levenberg-Maquardt least-squares algorithm routine of the OPUS software package, and the residual RMS error was about 0.001.

### 2D correlation analysis

A series of time-resolved spectra at equal time intervals and in a certain wavenumber range were selected for 2D correlation analysis using the “2D Shige” software developed by Dr.



**Scheme 1** Schematic illustration of the ATR-FTIR experimental configuration.

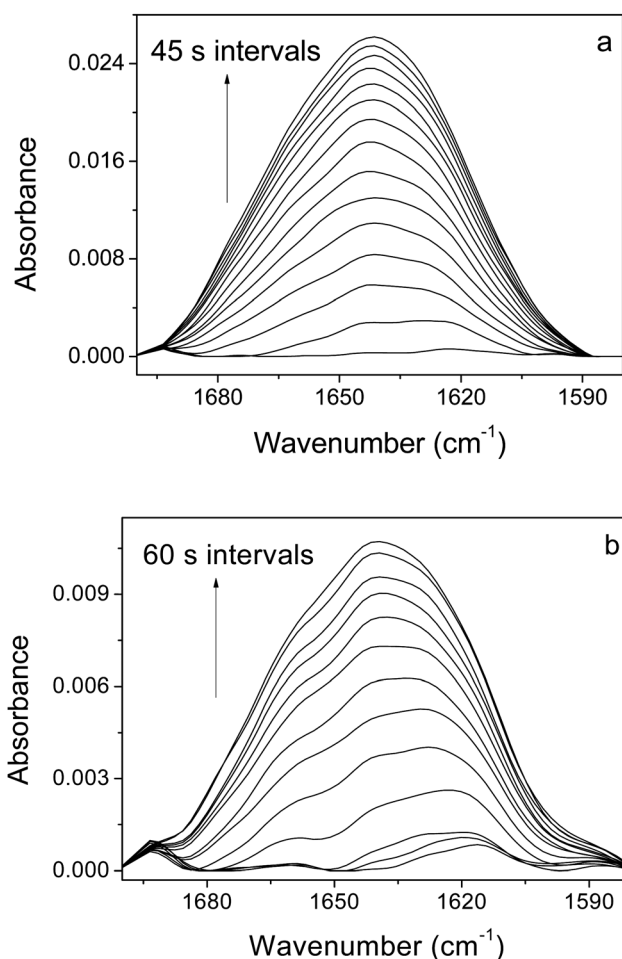
Shigeaki Morita (Ozaki group, Kwansai Gakuin University). In the 2D correlation maps, unshaded regions indicate positive correlation intensities, whereas gray-colored regions are negative ones.

## Results and discussion

The ATR-FTIR method can provide real-time information about water in a polymer film within a certain depth. For our ATR setup for water diffusion measurements, the penetration depth ( $d_p$ ) at 1600 cm<sup>-1</sup> (where the O–H bending absorption band occurs) was about 1.2 μm according to the following equation:  $d_p = \lambda / (2\pi n_1 (\sin^2 \theta - n_{21}^2)^{1/2})$ , where  $\lambda$  is wavelength of the radiation in air,  $\theta$  is the incidence angle,  $n_1$  the refractive index of the ATR crystal, and  $n_{21}$  the ratio of the refractive index of the polymer to that of the ATR crystal. The penetration depth was much smaller than the thickness of the film (>10 μm) and can be assumed to be constant during the diffusion measurements.<sup>22</sup> Both amorphous and semicrystalline PLA films were investigated and compared. The films cast from solution were amorphous, as indicated by DSC and FTIR analyses, whereas the films cast after isothermal crystallization were found to be semicrystalline, with a degree of crystallinity of ~34%, as determined by DSC (ESI†).

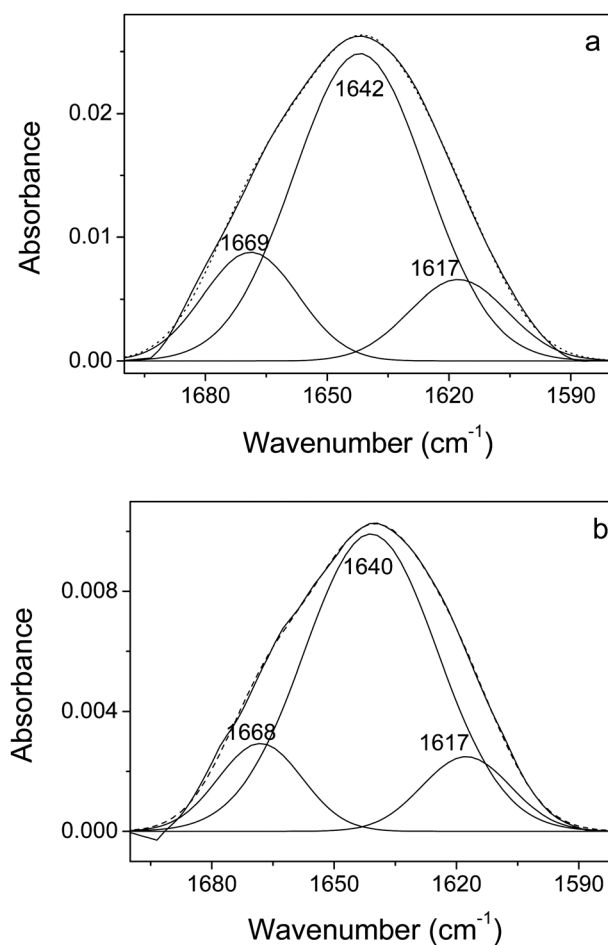
Time-resolved ATR-FTIR spectra in the range of 1700–1580 cm<sup>-1</sup> after baseline correction for the absorption of water into both PLA films are shown in Fig. 1. The infrared band, assigned to the O–H bending vibration of water ( $\delta_{(\text{OH})}$ ), is observed to gradually increase as a function of time when water diffuses into the film. The broad  $\delta_{(\text{OH})}$  band of water in this region is not overlapped by vibrational bands of the polymer. Peak fitting of the band is shown in Fig. 2, where three components located at around 1670, 1640, and 1620 cm<sup>-1</sup> are readily identified for both amorphous and crystalline PLA films. Because of the uncertainty in curve fitting processes, 2D correlation analysis was performed to validate these components.

Fig. 3 shows the 2D asynchronous correlation spectra of water absorbed in the two kinds of PLA films in the same spectral range of 1700–1580 cm<sup>-1</sup>. In this water diffusion study, all the synchronous cross-peaks are positive (ESI†). It can be seen from Fig. 3 that the broad O–H bending band comprises three separate components, located at ~1680, 1640, 1600 cm<sup>-1</sup> and ~1670, 1625, 1595 cm<sup>-1</sup> for amorphous and crystalline PLA films respectively, which are consistent with and support the above findings from peak fitting shown in Fig. 2. The peak fitting and 2D analysis results suggest that there are three different states of water in the film. The three components correspond to the absorbance from strongly hydrogen-bonded, moderately hydrogen-bonded, and weakly hydrogen-bonded hydroxyl groups, respectively. More specifically, the band at 1680 cm<sup>-1</sup>, the highest component, indicates strong hydrogen-bonding interactions between hydrophilic groups of the polymer and the water molecules, the bands at 1640 and 1625 cm<sup>-1</sup> are associated with moderate hydrogen-bonding interactions between the hydrophilic groups and the water molecules, and the absorption at the lowest frequency (1595 cm<sup>-1</sup>) belongs to the water molecules residing in free volume (microvoids) with little or no hydrogen bonding between each other (more detailed discussion on these structures in next section).



**Fig. 1** ATR-FTIR spectra measured during the absorption of water into amorphous (a) and crystalline (b) PLA films in the range of 1700–1580  $\text{cm}^{-1}$ .

In 2D correlation spectra,  $\phi(\nu_1, \nu_2)$  and  $\psi(\nu_1, \nu_2)$  represent the cross-peaks between  $\nu_1$  and  $\nu_2$  in synchronous and asynchronous correlation spectra, respectively.  $\phi(\nu_1, \nu_2)$  indicates the overall similarity between two separate spectral intensity variations measured at different spectral variables, while the appearance of an asynchronous correlation peak,  $\psi(\nu_1, \nu_2)$ , may be regarded as a measure of dissimilarity of the spectral intensity variations, and indicates that the bands  $\nu_1$  and  $\nu_2$  vary out of phase with each other during the diffusion process. The sign yields information about the sequential order of intensity changes between band  $\nu_1$  and band  $\nu_2$ . According to the rules proposed by Noda,<sup>29</sup> if  $\phi(\nu_1, \nu_2) > 0$  when  $\psi(\nu_1, \nu_2)$  is positive (unshaded area), band  $\nu_1$  varies before band  $\nu_2$  does, and when  $\psi(\nu_1, \nu_2)$  is negative (shaded area), it implies the opposite phenomena, that band  $\nu_1$  varies after band  $\nu_2$  does; if  $\phi(\nu_1, \nu_2) < 0$ , this rule is reversed. In the 2D synchronous correlation spectra of water absorbed in the two PLA films in the spectral range of 1700–1580  $\text{cm}^{-1}$ , the cross-peak is positive (Fig. S4, ESI†), which means that all the components increase with time during the diffusion process. In Fig. 3a, the positive  $\psi(1640, 1600)$  peak suggests that the band at 1640  $\text{cm}^{-1}$  varies prior to the band at 1600  $\text{cm}^{-1}$ , and the negative asynchronous cross-peak located at 1680/1640 reveals that the band at 1680  $\text{cm}^{-1}$  varies later than the band at 1640  $\text{cm}^{-1}$ .



**Fig. 2** Peak fitting of the infrared difference spectra of water in amorphous (a) and crystalline (b) PLA films in the range of 1700–1580  $\text{cm}^{-1}$ .

Therefore, the sequence of the spectral changes is obtained from asynchronous 2D ATR-FTIR correlation spectra by judgment of the sign of the correlation peak, which is as follows: 1640  $\rightarrow$  1680 and 1600  $\text{cm}^{-1}$ , for water diffusion in the amorphous PLA film. In Fig. 3b, the positive  $\psi(1625, 1595)$  peak suggests that the band at 1625  $\text{cm}^{-1}$  varies prior to the band at 1595  $\text{cm}^{-1}$ , and the negative asynchronous peak located at 1670/1625  $\text{cm}^{-1}$  reveals that the band at 1670  $\text{cm}^{-1}$  varies later than the 1625  $\text{cm}^{-1}$  band. Then the sequence of the spectral changes is as follows: 1625  $\rightarrow$  1670 and 1595  $\text{cm}^{-1}$ , for water diffusion in the crystalline PLA film. In addition, from the above 2D analysis results, it can be found that O–H bending for each state of hydrogen-bonded water in the amorphous film occurs at slightly higher wavenumbers than that in the crystalline film, which indicates that water is more confined in the ordered polymer segments of the crystalline PLA matrix. Furthermore, it is known that carbonyl can form moderately strong ( $-\text{CO}-\text{HOH}$  and  $-\text{CO}-\text{HOH}-\text{HOH}$ ), and strong hydrogen bonds ( $-\text{CO}-\text{HOH}-\text{CO}-$  and  $-\text{CO}-\text{HOH}-\text{HOH}$ ) with water.<sup>21,34</sup> By combining these structures with our analyses on the spectroscopic data discussed above, as shown in Fig. 4, we can conclude that when water diffuses into PLA films, it is moderately bound to the polymer first, by preferentially forming hydrogen bonds with the C=O group. Then, water molecules diffuse into free volume (microvoids) in the polymer matrix, forming water

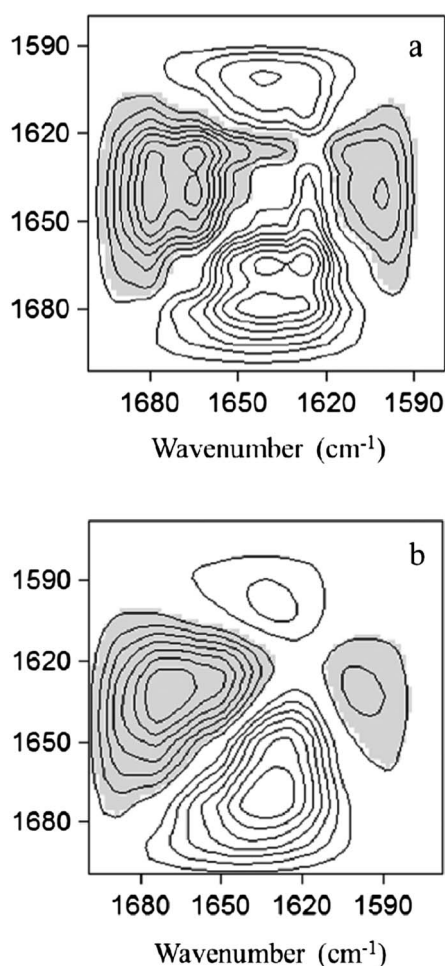


**Fig. 3** Asynchronous 2D FT-IR correlation spectra of water diffusion into amorphous (a) and crystalline (b) PLA films in the range of 1700–1580  $\text{cm}^{-1}$ .

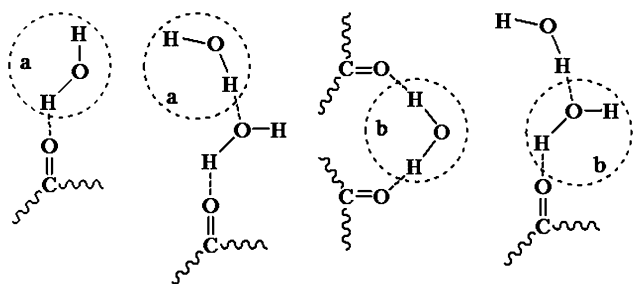


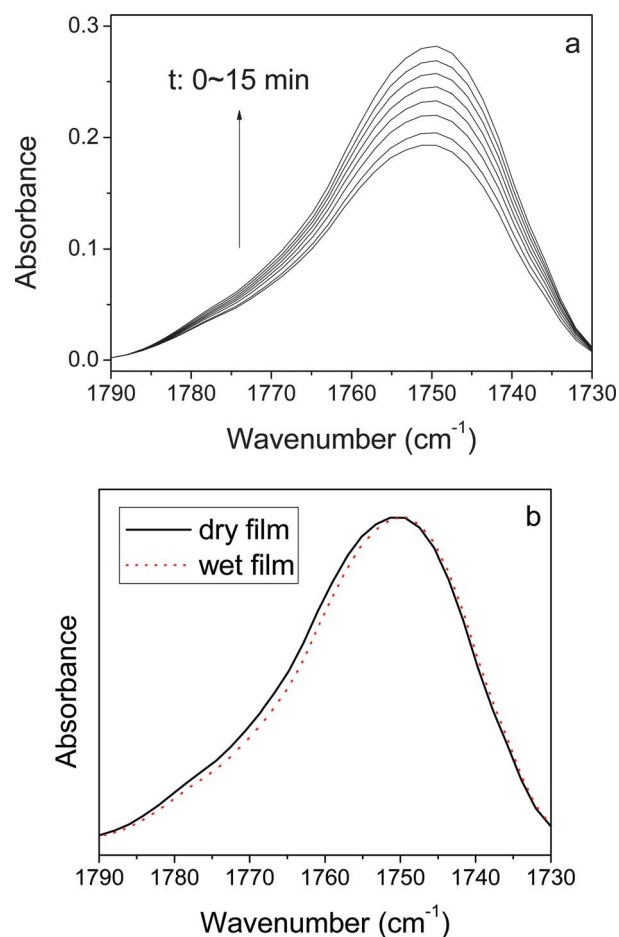
**Fig. 4** Interactions between water and poly(lactic acid): moderately strong (a) and strong (b) hydrogen bonds.

clusters, as well as into the polymer network, forming strong hydrogen bonds with the polymer.

After the various structures of water formed in the diffusion process have been identified, we turn to the effects of water on the polymer structure by studying the characteristic bands of PLA. According to the literature,<sup>36</sup> the carbonyl stretching band of PLA at 1790–1730  $\text{cm}^{-1}$  is composed of four components at about 1776, 1767, 1759, and 1749  $\text{cm}^{-1}$ . The bands at 1776, 1767, and 1749  $\text{cm}^{-1}$  are attributed to *gg*, *tg*, and *tt* conformers,

respectively, primarily due to intramolecular coupling, while the band at 1759  $\text{cm}^{-1}$  corresponds to the overlapped absorption of *gt* conformers in the amorphous and crystalline phases.<sup>36</sup> Fig. 5 shows the IR spectra in the carbonyl stretching region of the amorphous film as a function of water uptake. It can be seen that the shape of this carbonyl stretching band remains the same throughout the water uptake process, which is more obvious in Fig. 5b, where the spectra for the film in dry and wet states are compared on the same absorbance scale. These two spectra were fitted with the four components, and their area fractions are listed in Table 1. It is clear that the four components of the carbonyl stretching are essentially the same in dry and wet states, suggesting that the inclusion of water does not alter the conformation distribution of the amorphous polymer chains, even though water forms hydrogen bonds with the polymer.

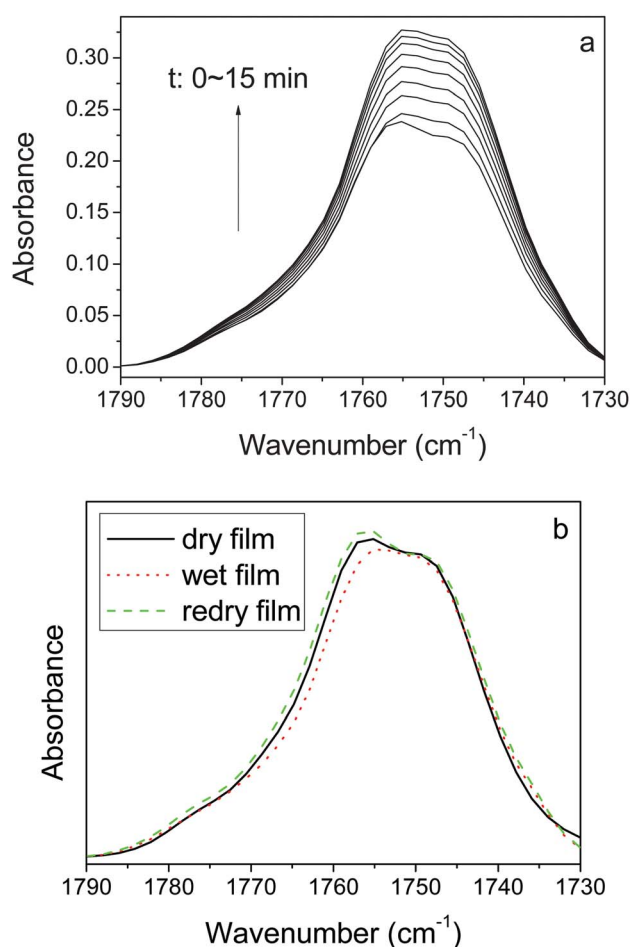
For the crystalline film, however, pronounced splitting and broadening of the carbonyl band, shown in Fig. 6a, is observed in both dry and wet states, presumably due to the addition of the crystalline component. Furthermore, the band broadening and splitting are reduced in the wet state compared to the dry one, as seen in Fig. 6b, suggesting a variation in conformation distribution in the crystalline film with water sorption. The composition of the carbonyl band was analyzed *via* band deconvolution, and the area fractions of the components are listed in Table 1. It



**Fig. 5** ATR-FTIR spectra in the 1790–1730  $\text{cm}^{-1}$  region for water diffusion into amorphous PLA film.

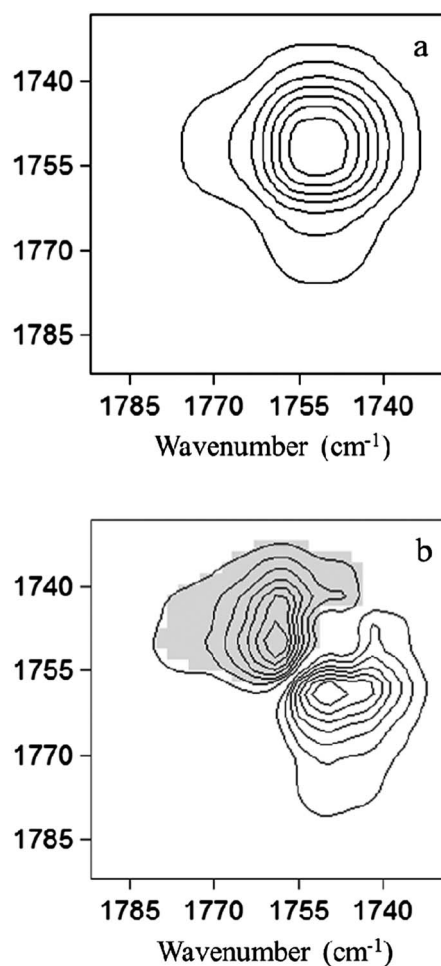
**Table 1** Peak fitting results of the carbonyl stretching region for amorphous and crystalline PLA films

Sample	State	Area fraction of component (%)			
		1776 $\text{cm}^{-1}$	1767 $\text{cm}^{-1}$	1758 $\text{cm}^{-1}$	1748 $\text{cm}^{-1}$
Amorphous film	Dry	7	12	17	64
	Wet	6	12	17	65
Crystalline film	Dry	4	10	26	60
	Wet	3	11	21	65
	Re-dried	4	10	26	60

**Fig. 6** ATR-FTIR spectra in the 1790–1730  $\text{cm}^{-1}$  region for water diffusion into crystalline PLA film.

is interesting to observe that the area fraction of the component at 1758  $\text{cm}^{-1}$ , associated with the crystalline phase, is 26% in dry state, and decreases to 21% after water uptake. Then upon re-drying of the wet film, the carbonyl band regains the shape of the dry state, and the area fraction of the component at 1758  $\text{cm}^{-1}$  rises to  $\sim$ 26% again. These results suggest that although the PLA crystalline region is difficult for water molecules to penetrate, part of the crystalline chains, probably the segments in the interphase between the crystalline and the amorphous domains, can still interact with the water molecules, resulting in a conformation change of the polymer chains which is reversible upon removal of the water. The synchronous and asynchronous 2D FTIR correlation spectra of the crystalline PLA film in the

range of 1790–1730  $\text{cm}^{-1}$  for the water diffusion process are shown in Fig. 7. The cross-peaks in the synchronous map are positive, while in the asynchronous map the peak at  $\psi(1758, 1748)$  is negative. This means that the component at 1748  $\text{cm}^{-1}$  changes before the one at 1758  $\text{cm}^{-1}$ . According to the assignments of the components of the carbonyl stretching band, it is evident that the amorphous carbonyl changes before the crystalline carbonyl does; *i.e.*, water molecules first form hydrogen bonds with the amorphous carbonyls and then diffuse into the crystalline domains and interact with the crystalline carbonyl groups.

**Fig. 7** Synchronous (a) and asynchronous (b) 2D FTIR correlation spectra for water diffusion into crystalline PLA film in the range of 1790–1730  $\text{cm}^{-1}$ .

## Conclusions

Water diffusion in PLA film has been investigated by 2D ATR-FTIR at a molecular level. There are three different states of water molecules in the film. Water first forms moderately strong hydrogen bonds with the carbonyls. Then, water diffuses into free volume, and water molecules become strongly bound *via* hydrogen bonding with  $\text{C=O}$  and water clusters. With absorption of water, the conformation distribution of crystalline PLA chains is disturbed, which can be reversed upon removal of the water; the conformation of amorphous PLA chains are not altered in the absorption process. These results demonstrate that morphology is critical to the diffusion of water in crystalline matrices and may help guide the design, processing, and application of PLA in various biomedical and pharmaceutical areas.

## Acknowledgement

Z.S. thanks the NSFC Fund for Creative Research Groups (50921062) for support.

## Notes and references

- 1 Y. Ikada and H. Tsuji, *Macromol. Rapid Commun.*, 2000, **21**, 117–132.
- 2 H. Tsuji and Y. Ikada, *Macromol. Chem. Phys.*, 1996, **197**, 3483–3499.
- 3 H. Tsuji and Y. Ikada, *J. Appl. Polym. Sci.*, 1998, **67**, 405–415.
- 4 H. Urayama, T. Kanamori and Y. Kimura, *Macromol. Mater. Eng.*, 2002, **287**, 116–121.
- 5 L. S. Nair and C. T. Laurencin, *Prog. Polym. Sci.*, 2007, **32**, 762–798.
- 6 B. Eling, S. Gogolewski and A. J. Pennings, *Polymer*, 1982, **23**, 1587–1593.
- 7 L. Fambri, A. Pegoretti, R. Fenner, S. D. Incardona and C. Migliaresi, *Polymer*, 1997, **38**, 79–85.
- 8 A. R. Postema and A. J. Pennings, *J. Appl. Polym. Sci.*, 1989, **37**, 2351–2369.
- 9 W. Hoogsteen, A. R. Postema, A. J. Pennings, G. Tenbrinke and P. Zugenmaier, *Macromolecules*, 1990, **23**, 634–642.
- 10 R. G. Sinclair, *J. Macromol. Sci., Pure Appl. Chem.*, 1996, **A33**, 585–597.
- 11 L. McEwan, R. A. Pethrick and S. J. Shaw, *Polymer*, 1999, **40**, 4213–4222.
- 12 M. Vert, S. M. Li and H. Garreau, *J. Biomater. Sci., Polym. Ed.*, 1994, **6**, 639–649.
- 13 P. Moy and F. E. Karasz, *Polym. Eng. Sci.*, 1980, **20**, 315–319.
- 14 C. Sammon, C. Mura, J. Yarwood, N. Everall, R. Swart and D. Hodge, *J. Phys. Chem. B*, 1998, **102**, 3402–3411.
- 15 M. Woo and M. R. Piggott, *J. Compos. Technol. Res.*, 1987, **9**, 101–107.
- 16 R. Auras, B. Harte and S. Selke, *Macromol. Biosci.*, 2004, **4**, 835–864.
- 17 R. A. Cairncross, J. G. Becker, S. Ramaswamy and R. O'Connor, *Appl. Biochem. Biotechnol.*, 2006, **131**, 774–785.
- 18 H. Tsuji and Y. Ikada, *Polym. Degrad. Stab.*, 2000, **67**, 179–189.
- 19 H. Tsuji, A. Mizuno and Y. Ikada, *J. Appl. Polym. Sci.*, 2000, **77**, 1452–1464.
- 20 J. S. Yoon, H. W. Jung, M. N. Kim and E. S. Park, *J. Appl. Polym. Sci.*, 2000, **77**, 1716–1722.
- 21 S. Cotugno, D. Larobina, G. Mensitieri, P. Musto and G. Ragosta, *Polymer*, 2001, **42**, 6431–6438.
- 22 G. T. Fieldson and T. A. Barbari, *Polymer*, 1993, **34**, 1146–1153.
- 23 M. J. Liu, P. Y. Wu, Y. F. Ding, G. Chen and S. J. Li, *Macromolecules*, 2002, **35**, 5500–5507.
- 24 Y. Marechal and A. Chamel, *J. Phys. Chem.*, 1996, **100**, 8551–8555.
- 25 D. Murphy and M. N. Depinho, *J. Membr. Sci.*, 1995, **106**, 245–257.
- 26 C. Sammon, C. Mura, S. Hajatdoost and J. Yarwood, *J. Mol. Liq.*, 2002, **96–97**, 305–315.
- 27 I. Noda, *Bull. Am. Phys. Soc.*, 1986, **31**, 520.
- 28 I. Noda, *J. Am. Chem. Soc.*, 1989, **111**, 8116–8118.
- 29 I. Noda, *Appl. Spectrosc.*, 1993, **47**, 1329–1336.
- 30 K. Murayama, Y. Q. Wu, B. Czarnik-Matusiewicz and Y. Ozaki, *J. Phys. Chem. B*, 2001, **105**, 4763–4769.
- 31 Y. Shen and P. Y. Wu, *J. Phys. Chem. B*, 2003, **107**, 4224–4226.
- 32 Y. Jin and Z. H. Su, *Chin. J. Appl. Chem.*, 2011, **28**, 16–21.
- 33 B. B. Tang, P. Y. Wu and H. W. Siesler, *J. Phys. Chem. B*, 2008, **112**, 2880–2887.
- 34 L. S. Wan, X. J. Huang and Z. K. Xu, *J. Phys. Chem. B*, 2007, **111**, 922–928.
- 35 W. Wang, Y. Jin and Z. H. Su, *J. Phys. Chem. B*, 2009, **113**, 15742–15746.
- 36 E. Meaurio, E. Zuza, N. Lopez-Rodriguez and J. R. Sarasua, *J. Phys. Chem. B*, 2006, **110**, 5790–5800.